SEMI-ANNUAL STATUS REPORT ON BOILING FLOW INSTABILITY

A. H. STENNING
T. N. VEZIROGLU

November 1965

MECHANICAL ENGINEERING DEPARTMENT
UNIVERSITY OF MIAMI
CORAL GABLES, FLORIDA

N 66-81112
(ACCESSION NUMBER)
40
(PAGES)
CR-69371
(NASA CR OR TMX OR AD NUMBER)
FACILITY FORM 602
(THRU)
(CODE)
(CATEGORY)

NASA GRANT NsG-424
REPORT NO. 8

SEMI-ANNUAL STATUS REPORT

ON BOILING FLOW INSTABILITY

November 1965

By A. H. Stenning and T. N. Veziroglu

INTRODUCTION

The two-phase flow instability studies carried out during the fifth six-monthly period can, in general, be divided into three groups; viz., (a) the study of density-wave two-phase flow oscillations in superheated Freon-11, (b) the study of pressure-drop two-phase flow oscillations in Freon-11, and (c) the measurement of slip in air-water two-phase flows. In addition, using the IBM 7040 Digital Computer of the University of Miami, an analytical study of the pressure-drop two-phase flow oscillations was undertaken. It is expected that this analytical work will be completed during the next six-monthly period.

It was found that the actual superheated Freon-11 flow systems were much more stable than those indicated by an analytical study [1]* of a homogeneous model. This could partly be accounted for by the strong dependence of the heat transfer coefficient in the boiling region on the mass flow rate.

A set of experiments were carried out to determine the

---

* The numbers in brackets refer to the references at the end of the Report.

steady state relationship between flow rate, heat input and pressure drop for the region of the pressure-drop two-phase flow oscillations. The experimental results have been correlated to obtain an equation between the three variables. Other experiments were carried out to study the pressure-drop two-phase flow oscillations as a continuation of the program started during the last six-monthly period. The results indicated that these oscillations may originate whenever the pressure drop versus mass flow rate for a given power input has a negative slope. Under certain circumstances, the density-wave two-phase flow oscillations are observed on part of the pressure-drop two-phase flow oscillation cycles.

Using a simple apparatus, the slip ratio (the ratio of gas velocity to liquid velocity) in downward air-water two-phase flows was measured. The results indicate that the slip ratio asymptotically approaches 1 as the overall density ratio (the inlet density divided by the exit density) increases. This explains why a homogeneous model was successful in predicting the onset of density-wave two-phase flow oscillations and their frequencies in the case of downward air-water two-phase flows [2].

DENSITY-WAVE OSCILLATIONS WITH SUPERHEAT

Apparatus

The apparatus used to investigate the density-wave two-phase flow oscillations in superheated Freon-11 is shown schematically in Fig. 1. The apparatus is a modified version

of the Freon-11 apparatus used to investigate the density-wave two-phase flow oscillations in boiling Freon-11. The test section consists of a surge tank, an inlet valve, a heater, an exit plenum, and an exit valve with some tubing in between to facilitate various connections. Most of the tubing in the system, including the heater, is made of nichrome with 0.1475 inch inside diameter and 3/16 inch outside diameter. The heater tube, 37 1/2 inches long, is itself used as the electrical resistance for providing heat input. D. C. voltage is applied at the ends of the heater tube, and power input up to 5 k.w. can be obtained with a maximum current of 200 amperes. In order to reduce the heat losses to a minimum, a vacuum jacket is built around the heater, which contains a radiation guard. The vacuum jacket is connected to a vacuum pump to evacuate air and other gases. At the inlet side of the heater a sight glass tube is included in the system to make sure that no evaporation starts in the liquid Freon-11 before reaching the heater. The surge tank was installed to reduce the severity of the pressure oscillations, which in early experiments without the surge tank had damaged several pressure gauges. It is made of stainless steel (4 inches diameter x 9 inches height) with a glass tube level indicator at the side and a bicycle type check valve at the top. The check valve was used for pumping in air as needed, since it was found that the trapped air would flow out through the system in between the experiments and be

replaced by Freon-11 vapor which in turn would condense during the experiments as pressures were increased. In order to decrease the possibility of air escape, a 1/8 inch thick and 3 7/8 inch diameter lucite disc was used as a float on the free Freon-11 surface in the surge tank. The exit plenum (7 inches long x 4 inches diameter) was placed at the downstream end of the heater to simulate the geometry of nuclear rocket engines. The exit plenum was connected to a 5/8 inch diameter exit pipe - in which the pressures were atmospheric - through a 5 inch long and 0.185 inch inside diameter nichrome tube and a needle valve. Two flow-through copper-constantan thermocouples were inserted into the system before and after the heater to measure the temperatures of Freon-11. Five copper-constantan thermocouples were fixed to the outer wall surface of the heater to measure heater wall temperatures. They were electrically insulated from the heater by means of 0.0015 inch thick mica flakes. Three bourdon type Heise pressure gages and two strain gage type pressure transducers were installed in the test section to measure the pressures at various stations across the system, and sense the pressure oscillations. A differential pressure transducer, Sanborn Model 270, was installed at the upstream side of the heater to record the instantaneous flow rates and sense the flow oscillations. The outputs from the pressure and differential pressure transducers were recorded on a two-channel Sanborn chart recorder.

The experimental set up included a Freon-11 container at the upstream side of the test section, and the Freon-11 recovery system at the downstream side. The Freon-11 container has a volume of 4 cubic feet and is made of stainless steel to withstand pressures up to 150 p.s.i.g. During the experiments Freon-11 in the container is pressurized by means of high pressure nitrogen and a constant pressure regulating valve to maintain flow into the test section, via a filter, a micrometer control valve, and a rotameter. Superheated Freon-11 leaving the test section is led into the recovery system. This system is essentially a heat exchanger where Freon-11 is condensed by making it run through a helical aluminum tube around which refrigerated brine at $32^{\circ}F$ circulates. The liquefied Freon-11 is then stored in a tank for re-use.

Experimental Procedure

In the experiments for determining the onset of density-wave two-phase flow oscillations with superheated Freon-11 and the influence of the various factors affecting the oscillations, first liquid Freon-11 was run through the system with the inlet valve partly closed and the exit valve fully open, after pressurizing the Freon-11 in the container up to about 50 to 70 p.s.i.g. by means of nitrogen gas. The regulator valve kept the tank pressure constant within $\pm$ 0.1 p.s.i. during the experiments. Then the heater was started at a relatively low power level of about 100 watts. Its power was then

increased to a predetermined test level by 50 watt increments. After each change in power, about 10 minutes was allowed to elapse before the next change. This procedure prevented unwanted transient instabilities. During the heater power level increases the Freon-11 flow rate was increased by adjusting the control valve and the pressure drop upstream of the heater was increased (if necessary) by adjusting the inlet valve so that the system was always operating within the stable zone at steady state. After the test power level was reached, the Freon-11 flow rate was adjusted by means of the control valve so as to obtain a few degrees (about $5^{o}F$) of superheated Freon-11 at the heater exit. During this procedure the inlet valve opening was reduced if necessary to obtain a steady flow. Then the inlet valve was slowly opened till the onset of density-wave two-phase flow oscillations was noticed. These oscillations could be observed from the periodic motion of the pressure gage pointers and also from the pressure and flow rate recordings. Since the experiments indicated that there was no noticeable hysterisis effect, the stability boundary was always reached from the stable zone as this procedure resulted in some time saving. At the stability boundary the room temperature, barometric pressure, Freon-11 mass flow rate, heater voltage and current, and pressure and temperature (thermocouple) readings at various stations along the test system were recorded. The above mentioned procedure was repeated by reducing the Freon-11

mass flow rate in steps by means of the control valve to obtain greater degrees of superheat. Then the experiments were repeated for other exit valve settings and for other power levels. Heater power level and Freon-11 mass flow rate combinations were so arranged that at all times the Freon-11 leaving the heater was superheated. The liquid Freon-11 temperatures at the heater inlet ranged from $70^{o}F$ to $76.6^{o}F$ for the superheat experiments.

Results and Discussion

Analyses made earlier [1] indicate that the parameters affecting the onset of density-wave two-phase flow oscillations with superheat, are overall density ratio (the inlet density of the liquid divided by the exit density of the superheated vapor) $1/r_{4s}$, density ratio over the boiling region (the inlet density of liquid divided by the saturated vapor density at the completion of boiling) $1/r_{3s}$, heat input fraction expended in removing subcooling c, fraction of heat transfer independent of mass flow rate b, inlet pressure drop fraction (system inlet to heater inlet pressure drop divided by the overall system pressure drop) y, inlet dynamic pressure $(\rho_1 u_1^2/2)$ divided by the overall system pressure drop p_d, normalized exit plenum pressure (exit plenum pressure divided by the overall system pressure drop) p_{4s}, exit plenum pressure divided by exit pressure p_{4s}/p_5, normalized exit plenum volume (exit plenum volume divided by the heater volume portion where boiling is completed) v_4, normalized

inlet ducting length (inlet tubing length divided by length of the heater portion over which boiling is completed) ℓ_o, and normalized heater length (heater length divided by the length of the heater portion over which the boiling is completed) ℓ_h. Using the experimental readings and the recordings, the above stated parameters were calculated. The calculations indicated that the fraction of heat transfer independent of mass flow rate was about 0.55 to 0.60 for all the onset conditions.

Because of the interdependence of the parameters affecting the stability boundary, it was not possible to keep all but two constant and investigate the relationship between them. Under the circumstances, in order to reduce the number of variables, first the overall density ratios ($1/r_{4s}$) were plotted against the mass flow rates $\dot{m}$ at constant power levels for varying exit valve settings (Fig. 2). As can be seen from Fig. 2, points corresponding to a certain heat input and system geometry as defined by the exit valve setting fall on smooth curves. Each exit valve setting resulted in a constant exit plenum pressure to heater inlet pressure ratio at stability onset points irrespective of the flow parameters. Hence, this ratio will be used to distinguish each exit valve setting. The curves plotted in Fig. 2 are in fact operating curves for each valve setting used. Then the points corresponding to a constant $1/r_{4s}$ were selected and the inlet fraction of pressure drop y and the mass flow rate $\dot{m}$ were

determined at the onset of instability for each such point. In order to keep $1/r_{4s}$ constant, some of the points were found by interpolation between two nearest onset points. The results are plotted for various combinations of $1/r_{4s}$ and the exit plenum pressure to the heater inlet pressure ratio P_{4s}/P_{1s} (Fig. 3). The region above each curve is stable and below unstable. From a study of Fig. 3, it can be seen that (1) increase in overall density ratio decreases stability, (2) increase in inlet fraction of pressure drop increases stability, (3) increase in exit plenum to heater inlet pressure ratio decreases stability, and (4) increase in mass flow rate decreases stability. The experiments also showed that for a given mass flow rate, the corresponding stable points had higher inlet pressure drop fractions than that of the onset point, and the unstable points had lower inlet pressure drop fractions.

When compared with the analyses, the actual systems with superheat seem to be much more stable. This can only partly be accounted for by the relatively strong dependence of boiling heat transfer on mass flow rate. Consequently, the results suggest that the slip ratio - which was neglected in the analytical studies - should have a strong stabilizing effect.

PRESSURE-DROP OSCILLATIONS

Apparatus

In the experiments to investigate the pressure-drop two-phase flow oscillations, the apparatus described in the last section was used with some modifications. Fig. 4 shows the modified apparatus schematically. As can be seen from the figure, the modifications consisted of (a) the omission of the exit plenum, (b) the replacement of the exit valve by an orifice, and (c) the inclusion of a constant temperature water bath.

The reason for the exclusion of the exit plenum was to reduce the number of variables. In replacing the exit valve by an orifice two purposes were served. The change produced a fixed system geometry which could be maintained over a long period of time, (much more so than was possible with a valve), and also made it possible to generate data to investigate two-phase flow orifice characteristics. Several orifices of different diameters were tried in order to find the one best suited to the study of the pressure-drop two-phase flow oscillations, i.e., the one producing the maximum negative slope in the plots of pressure drop versus mass flow rate. Finally a sharp edged orifice of 0.059 inch diameter was selected, and used throughout the experiments. Since some preliminary tests showed that it was important to keep the inlet temperature of Freon-11 constant to obtain repeatable results and since the laboratory temperatures were changing

by about $5^{o}F$ during a day (even though air conditioned), the constant temperature water bath mentioned above was installed in the system between the Freon-11 container and the surge tank. It consisted of a heat exchanger in which Freon-11 flowing through finned stainless steel tubing was brought down to a constant temperature by city water (whose temperature remained constant within $\pm$ $0.5^{o}F$) circulating around the finned tubing. As a result, the liquid Freon-11 temperature entering the heater was nearly constant for all the pressure-drop experiments and equal to 78.4 ± 0.6 ^{o}F. Also an x-y plotter was included in the experimental set-up to plot the pressure drop against flow rate directly.

Experimental Procedure

In the experiments for investigating the pressure-drop two-phase flow oscillations, first the constant temperature bath water supply was started and then the same procedure as described in the last section was followed up to the point of obtaining the test power level in the heater. After the test power level was reached, the Freon-11 flow rate was brought up to the maximum possible by opening both the control and the inlet valves. At this stable point the room temperature, barometric pressure, Freon-11 mass flow rate, heater voltage and current, and pressure and temperature (thermocouple) readings at various stations along the test system were recorded. Also the state point, as defined by the signals from the inlet pressure transducer and the mass flow rate

(differential pressure) transducer, was recorded on the x-y plotter. After this, the same procedure was repeated while reducing the Freon-11 mass flow rate (by closing the control valve) in steps. In all of these tests the system was kept stable (both with regard to the pressure-drop and the density-wave two-phase flow oscillations) by partially closing the inlet valve as needed. After completing the steady state experiments for a given heater power level as described above, the Freon-11 mass flow rate was increased to a value in which the pressure-drop two-phase flow oscillations were first noticed during the steady state experiments, i.e., the point where it was necessary to use the inlet valve to obtain stable flow. Then the inlet valve was completely opened and the resulting pressure-drop two-phase flow oscillations were recorded both on the strip chart and x-y recorders as pressure and mass flow rate versus time, and inlet pressure versus mass flow rate respectively. This procedure was then repeated by reducing the Freon-11 mass flow rate in steps till the disappearance of the pressure-drop two-phase flow oscillations or the appearance of the superposed density-wave two-phase flow oscillations.

The above described procedures for both the steady state and the unsteady state experiments were repeated for various heater power inputs. Also one set of experiments was run with no heater power input to obtain the lower bound of the steady state pressure drop versus mass flow rate relationships.

Results and Discussion

Fig. 5 shows the results of the steady state experiments plotted as the pressure drop between the inlet pressure transducer and the exit pipe versus Freon-11 mass flow rate for various heater power inputs. These curves, with one maximum and one minimum each, are similar to the usual forced convection boiling heater pressure drop versus mass flow rate relationships. After making a correction for the pressure drop between the surge tank and the inlet pressure transducer, these curves were correlated, and the following experimental state equation giving the relationship between the overall pressure drop between the surge tank and the exit, Freon-11 mass flow rate and the heater power input was obtained:

For $\dot{m}\, H^{-0.36} \leq 0.3$

$$\Delta P_{sy} = 2.85\, \dot{m}^2 + H^{1.3}\left\{0.02[1-\exp(-30\, \dot{m}H^{-0.36})]-0.06\, \dot{m}H^{-0.36}\right\}$$

and for $\dot{m}\, H^{-0.36} > 0.3$ ..(1)

$$\Delta P_{sy} = 2.85\, \dot{m}^2 + 13.11\, H^{1.3}\, \exp(-29.2\, \dot{m}\, H^{-0.36})$$

where,

Δp_{sy} = system pressure drop in p.s.i.

$\dot{m}$ = Freon-11 mass flow rate in lbs. $min.^{-1}$

H = heater power input in watts.

This equation is of course valid only within the ranges of the

experiments, i.e., up to 32 p.s.i. pressure difference, 3.2 lb. $min.^{-1}$ Freon-11 mass flow rate and 500 watts heater power input. This state equation is now being used in an analytical study of the pressure-drop two-phase flow oscillations.

Figs. 6 to 10 show the pressure-drop oscillation limit cycles (in some cases combined with density-wave oscillations) plotted directly on the pressure drop-flow rate plane at various operating points and for various heater power inputs. On these figures, also the corresponding steady state curves are shown. From a study of these figures and various variables recorded during the experiments, the following conclusions have been arrived at:

1. The pressure-drop two-phase flow oscillations may take place for operating points on the negative slope branch of the pressure drop versus mass flow rate curves provided that the system inlet pressure drop is low enough. For the system geometry investigated the pressure-drop two-phase flow oscillations (with or without superimposed density-wave two-phase flow oscillations) were obtainable whenever the pressure drop versus mass flow rate curve had a negative slope greater than 1.1 p.s.i./lbs.$min.^{-1}$ to 0.4 p.s.i./lbs.$min.^{-1}$ for heater inputs ranging from 1015 Btu/hr. to 1280 Btu/hr respectively. Because of the tubing between the surge tank and the heater inlet, the system always had a finite inlet pressure

drop. The density-wave two-phase flow oscillations would always take place for the operating points having zero or positive slopes on the two-phase portion, that is the portion leading from the origin, of the pressure drop versus mass flow rate curves, again provided that the inlet pressure drop was low enough.

2. The size (the pressure drop and mass flow rate amplitudes) of the pressure-drop two-phase flow oscillation limit cycles are small for the operating points near the minimum of the pressure drop versus mass flow rate curves. They grow as the operating point is moved up the negative slope branch towards larger negative slopes, and - with the exception of cases where the density-wave two-phase flow oscillations become superposed - they tend to become smaller again as the operating point nears the maximum pressure drop and the slope (though still negative) decreases in magnitude.

3. Because of the relatively large time period of oscillations, the pressure-drop two-phase flow oscillations are quasi-steady state phenomenon. At every instant of the limit cycles, the system state point as defined by the pressure drop, the mass flow rate and the heat input from the tube, moves on the steady state equilibrium surface (Fig. 5) defining the relationship between the above variables. Hence, the heat input to

the fluid is changing during the cycle, even though the electrical power input is constant. Thermal energy is stored in and released from the heater during each cycle, and the tube wall shows a corresponding temperature fluctuation of 2 to 4°F.

4. The time period of the pressure-drop two-phase flow oscillations varied from 42 seconds to 73 seconds. With the exception of the 1110 Btu/hr. heat input experiments where the time periods of the oscillations were nearly constant for all the limit cycles at about 51 seconds, the time periods increased as the steady-state operating points moved to lower mass flow rates.

5. Whenever the minimum flow attained in a limit cycle falls below the flow rate corresponding to the maximum pressure drop for the given power input, density-wave oscillations appear as a superimposed transient on the limit cycle (for example see Figs. 8 and 9) since at those points the overall density ratios are high enough to give rise to them. The superposition of the density-wave two-phase flow oscillations would slightly decrease the time periods of the pressure-drop limit cycle oscillations.

6. The pressure-drop two-phase flow oscillations could always be stopped by increasing the inlet pressure drop just as in the case of the density-wave two-phase flow oscillations.

Fig. 11 shows the orifice pressure drop versus mass flow rate relationships for two-phase Freon-11 flows for various heater power inputs and exit qualities. These experimental results have been correlated to obtain the following orifice equation for two-phase Freon-11 flow through sharp edged 0.059 inch diameter orifices, when the downstream pressure is atmospheric:

$$\Delta P_{or} = 1.85 \ (1 + 45x)^{1.3} \ \dot{m}^2 \qquad \ldots\ldots\ (2)$$

where,

Δp_{or} = orifice pressure drop in p.s.i.

$\dot{m}$ = Freon-11 mass flow rate in lbs. $min.^{-1}$

and x = quality.

As can be seen, the equation agrees with the well known square law applicable to liquids and gases.

SLIP IN AIR-WATER FLOWS

Apparatus

The apparatus used to investigate the slip, the ratio of gas velocity to liquid velocity, in air-water two-phase flows is shown schematically in Fig. 12. It consisted of water and air supply systems, a mixer and a test section with various measuring instruments. A constant level tank, a motor driven centrifugal pump, a control valve, a surge tank and an inlet valve made up the water supply system. The water supply system was so designed that water flow could be kept steady irrespective of the pressure fluctuations in

the city water mains. A Potter turbine type flow meter was included in the water system downstream of the surge tank to measure water mass flow rates. The air system started at the compressed air system in the laboratory and included a needle valve type control valve and a Vol-O-Flow flow meter. Because of the constant pressure of the compressed air system, the air flow rates could be kept steady. The mixer was made of a porous bronze tube of 5/8 inch inside diameter and 6 1/2 inches long, surrounded by an air chamber of 1 inch radial width. One end of the porous bronze tube was connected to the water supply system and the other end connected to the test section while the air chamber was connected to the air supply system.

The test section was made of a vertical clear lucite tube of 5/8 inch inside diameter and 26 inches long. It was fitted with two ball valves of 3/4 inch opening diameter, one at each end. The two ball valves were connected with a parallelogram mechanism with one handle so that both the valves could be operated simultaneously. A 90^{o} turn was enough to change the position of the valves from "open" to "closed" or vice-versa. The upstream side of the test section was connected to the mixer and the downstream side was connected to a plastic tube having an inner diameter of 5/8 inch, which had a 3/16 inch diameter round edged exit orifice clamped to it. The position of the exit orifice could be changed up to 2 feet from the test section in order to investigate the orifice entrance effect on slip.

Several Bourdon type pressure gages were placed along the water and air systems and the test section in order to measure water, air and mixture pressures.

Experimental Procedure

In experiments to investigate the slip in the air-water two-phase flow, air was first run through the system at a low flow rate, and then the water pump was started with test section valves in the open position. This prevented water from entering the air jacket. After this, the water flow rate was brought up to a predetermined value by adjusting the water control valve. The pressurized air supplied to the jacket of the mixer seeped through the porous bronze tube and bubbled into the water passing through the tube. The two-phase mixture formed in the mixer then flowed through the test section and out of the exit orifice. The flow observed in the test section was well mixed and bubbly.

After making sure that the air and water flow rates were steady, room temperature, barometric pressure, air and water flow rates and the pressures at various stations were recorded. Soon after taking the readings, the two test section valves were closed simultaneously by means of the parallelogram mechanism. (The surge tank eliminated the water hammer action which otherwise would have resulted from abrupt closing of the ducting.) After the separation of air and water in the test section, the water level was noted. This procedure was repeated for increasing air flow rates up to the onset of the

density-wave two-phase flow oscillations, by re-adjusting the water control valve at each step so that the water flow rate was kept constant. The experiments were not carried into the unstable region, since it was then not possible to obtain a uniform mixture in the test section.

The above described procedure was repeated for various water flow rates. In all the experiments the inlet valve was kept fully open.

Some preliminary tests were run with the exit orifice placed at distances varying from 2 inches to 2 feet from the downstream valve of the test section. No noticeable effect on slip was observed.

Results and Discussion

Using the readings taken during each experiment, the void fraction, the density ratio of the water density to that of the mixture and the slip (i.e., the ratio of gas velocity to liquid velocity) were calculated. The results are plotted in Figs. 13 and 14 as slip versus density ratio and slip versus void fraction respectively. From Fig. 13 it can be seen that for a downward air-water two-phase flow (a) the slip decreases and tends asymptotically towards one as density ratio increases, and (b) the slip decreases as liquid (in this case water) flow rate increases. Because of a directly varying relationship between the void fraction and the density ratio, the above observations also apply to the slip versus void fraction relationship (see Fig. 14).

In the instability experiments with the air-water two-phase flows [2], the density ratios at the onset of instabilities ranged from 3 to 11. From Fig. 13, it can be seen that for this density ratio range, the slip would be of the order of one (between 1 and 1.5). This then explains why the two-phase flow oscillations (density-wave type) theory [2] based on a homogeneous two-phase flow model gave good agreement with the experiments in predicting the instability onset parameters and frequencies.

REFERENCES

1. Stenning, A.H. and Veziroglu, T.N.: "Semi-Annual Status Report on Boiling Flow Instability," NASA Grant NsG-424, Report No. 3, May 1964.

2. Stenning, A.H. and Veziroglu, T.N.: "Oscillations in Two-Component Two-Phase Flow," ASME paper 65-FE-24 presented at the Applied Mechanics and Fluids Engineering Conference, June 1965.

NOMENCLATURE

H	Heater input.
ℓ	Ducting length divided by length of heater part over which the boiling is completed.
$\dot{m}$	Mass flow rate.
p	Pressure normalized with respect to system pressure drop.
P	Pressure.
r	Local density divided by inlet density.
s	Slip, gas velocity divided by liquid velocity.
u	Velocity.
v	Volume divided by volume of heater portion over which the boiling is completed.
x	Quality.
y	System inlet to heater inlet pressure drop divided by system pressure drop.
Δ	Difference.
ρ	Density.

Subscripts:

d	Dynamic.
h	Heater.
or	Orifice.
s	Stability onset.
sy	System.
o	System inlet to heater inlet.
1	Heater inlet.
3	End of boiling region.
4	Exit plenum.
5	System exit.

LIST OF FIGURES

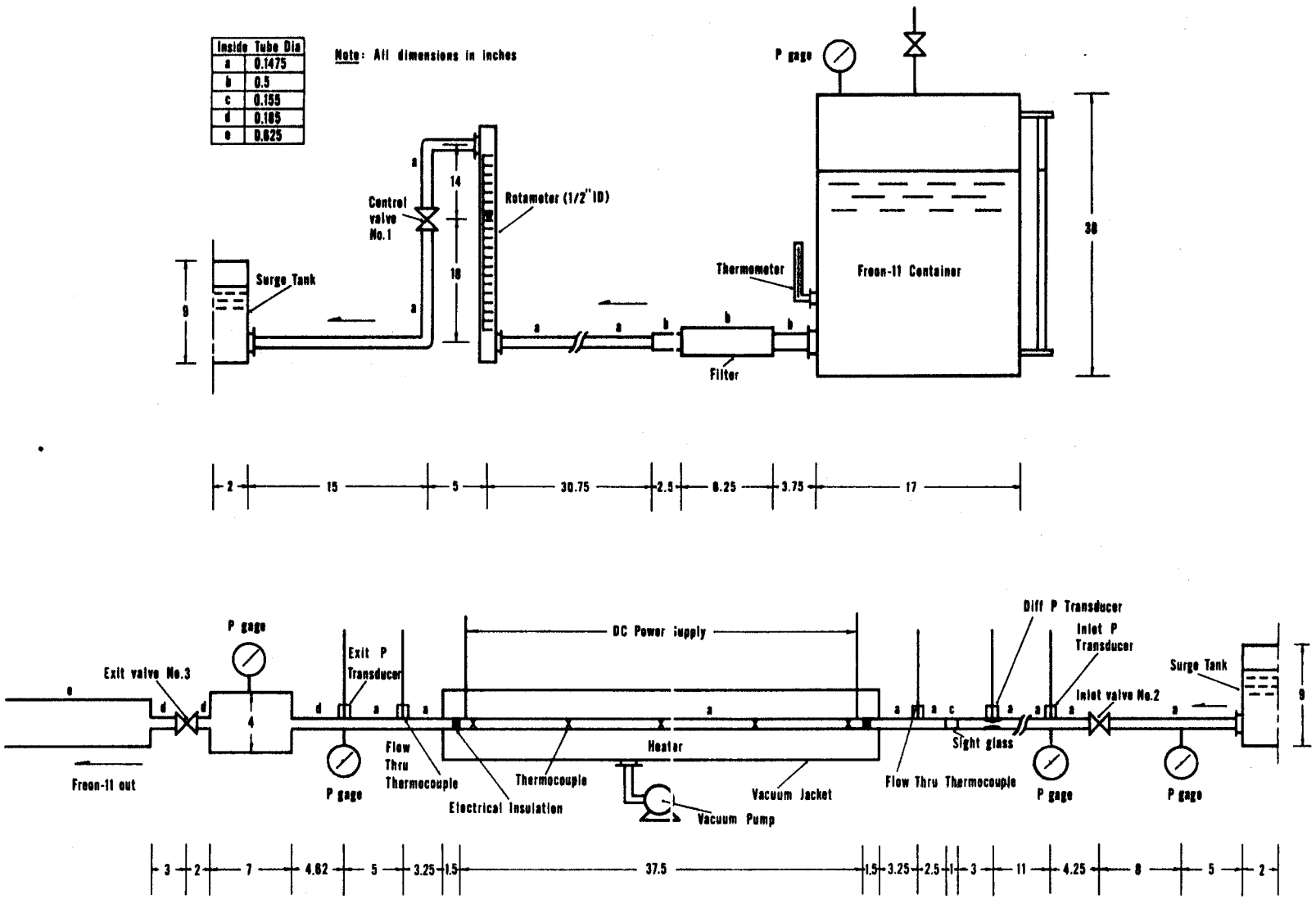

FIG. 1.- SCHEMATIC DIAGRAM OF EXPERIMENTAL SET-UP FOR DENSITY-WAVE OSCILLATIONS WITH SUPERHEAT

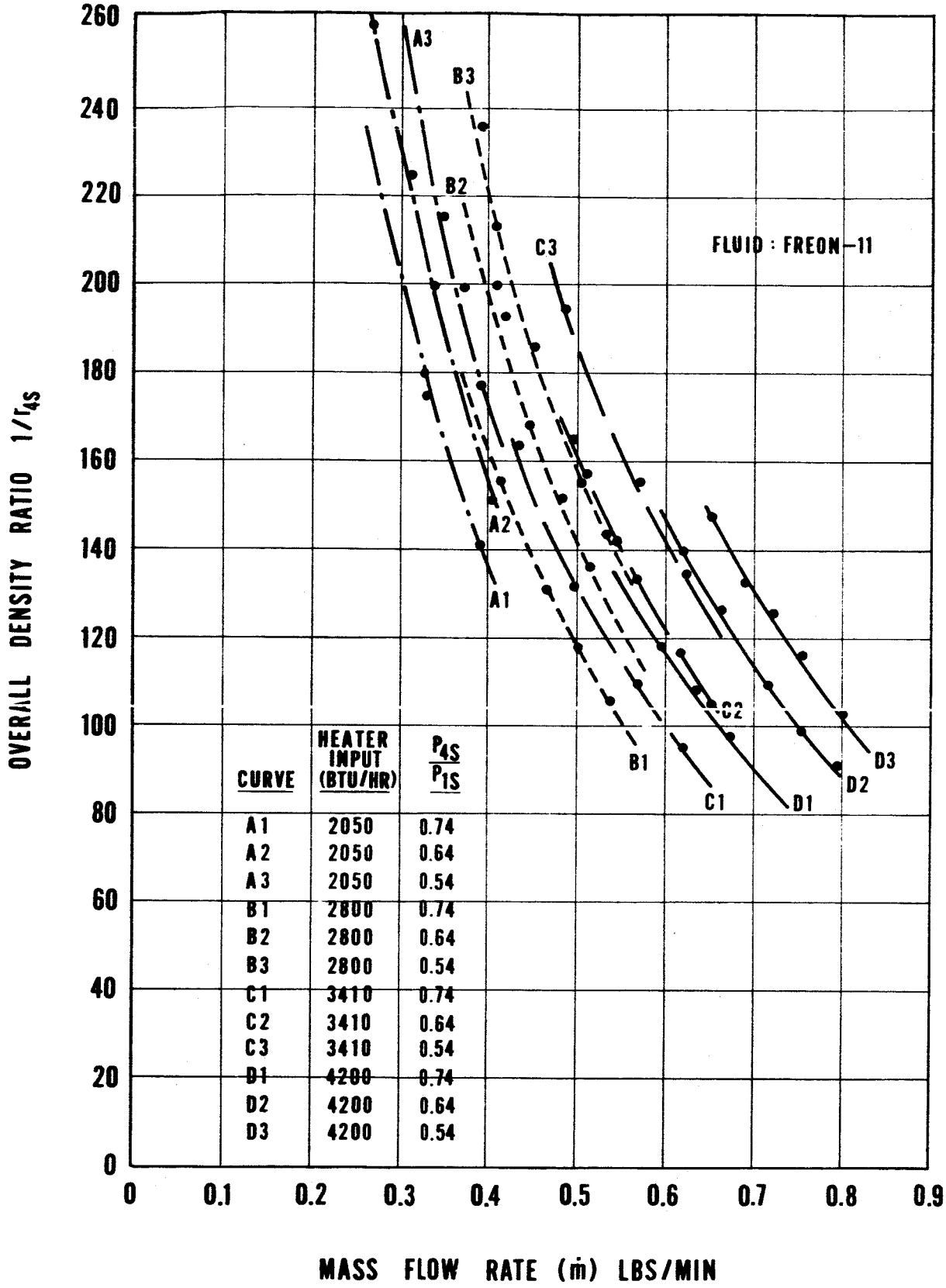

CURVE	HEATER INPUT (BTU/HR)	$\frac{P_{4S}}{P_{1S}}$
A1	2050	0.74
A2	2050	0.64
A3	2050	0.54
B1	2800	0.74
B2	2800	0.64
B3	2800	0.54
C1	3410	0.74
C2	3410	0.64
C3	3410	0.54
D1	4200	0.74
D2	4200	0.64
D3	4200	0.54

FIG. 2.– OVERALL DENSITY RATIO VS MASS FLOW RATE FOR SUPERHEAT EXPERIMENTS

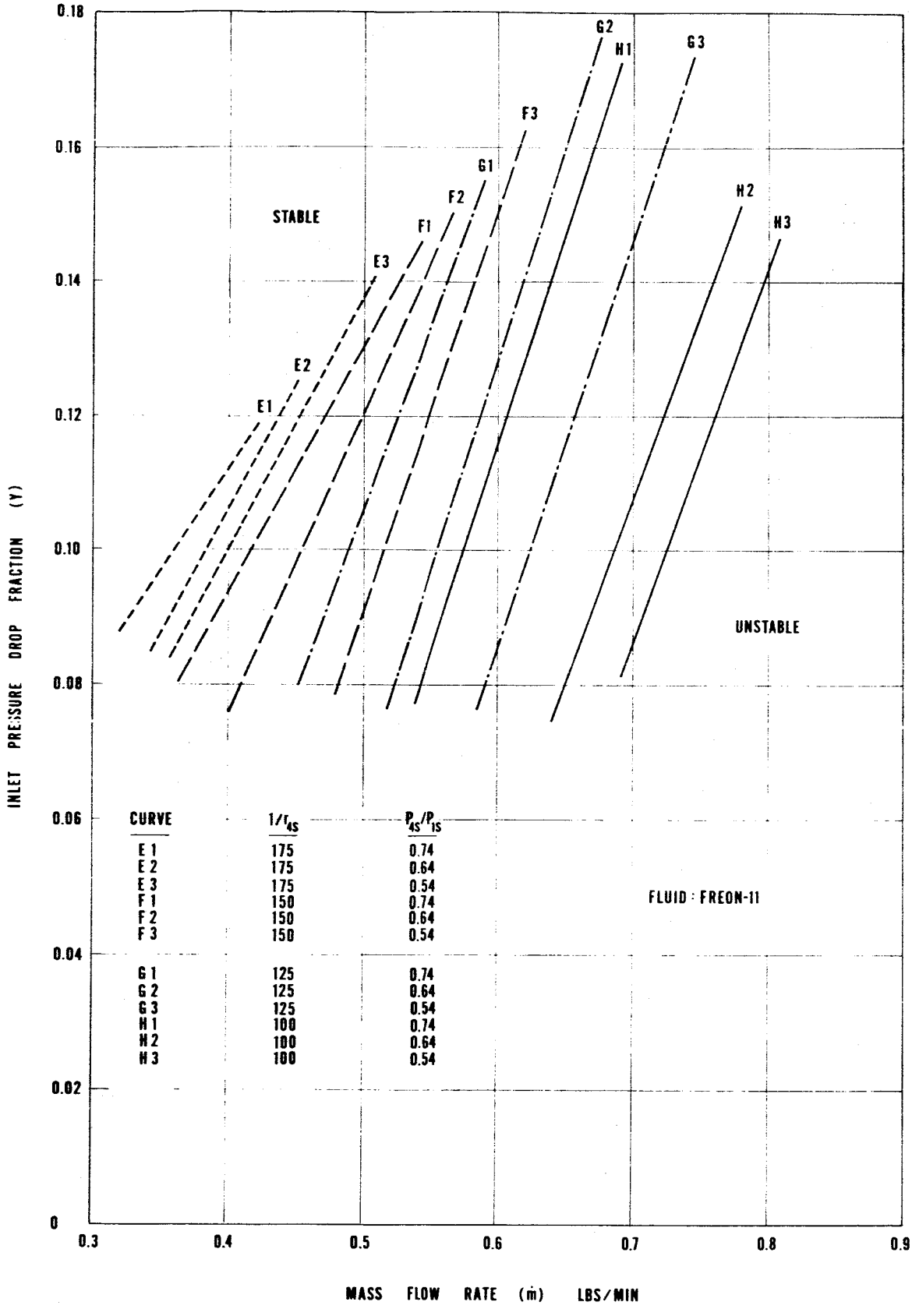

FIG. 3. – INLET PRESSURE DROP FRACTION VS MASS FLOW RATE AT STABILITY BOUNDARY FOR SUPERHEAT EXPERIMENTS

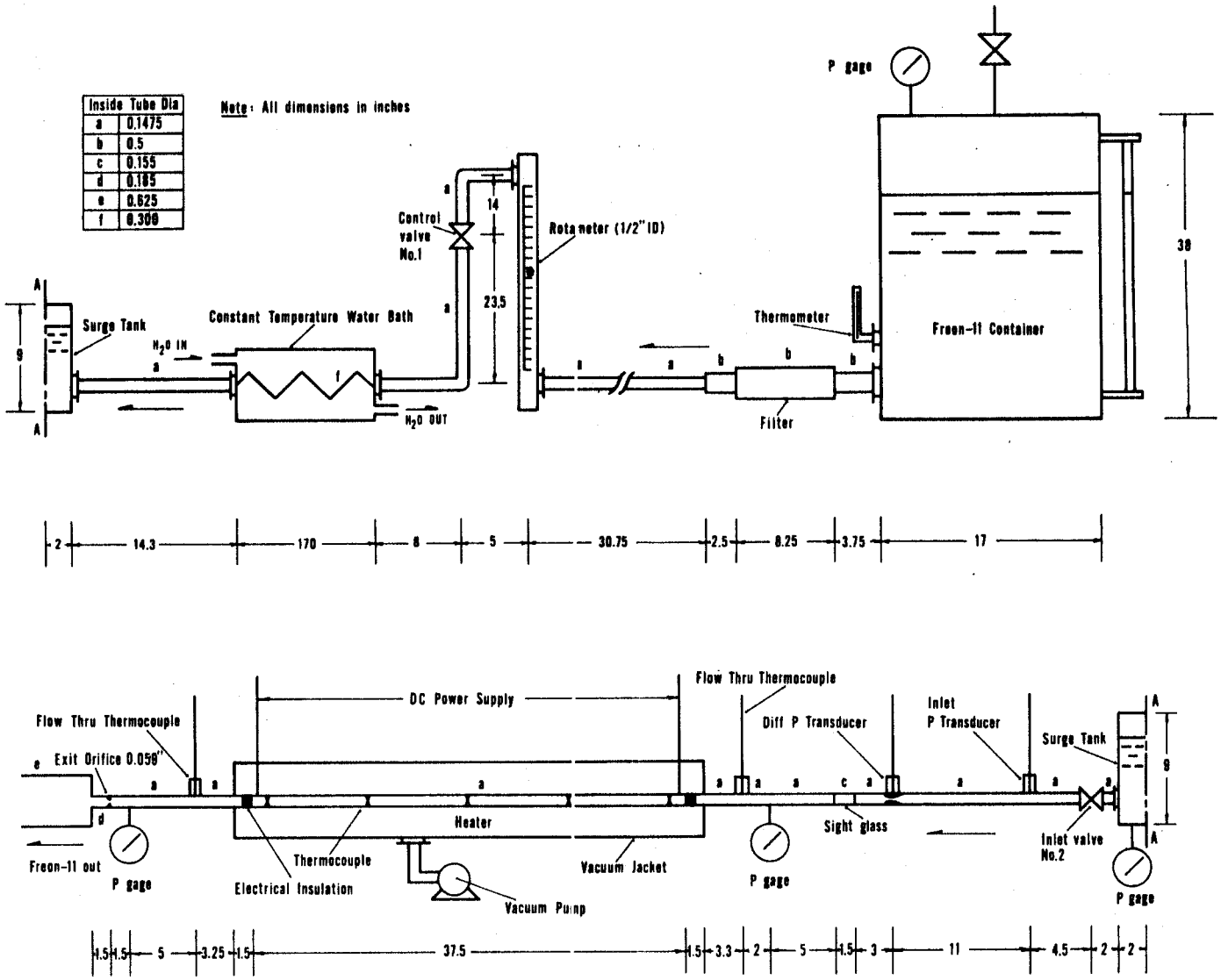

FIG. 4.- SCHEMATIC DIAGRAM OF EXPERIMENTAL SET-UP FOR PRESSURE-DROP OSCILLATIONS

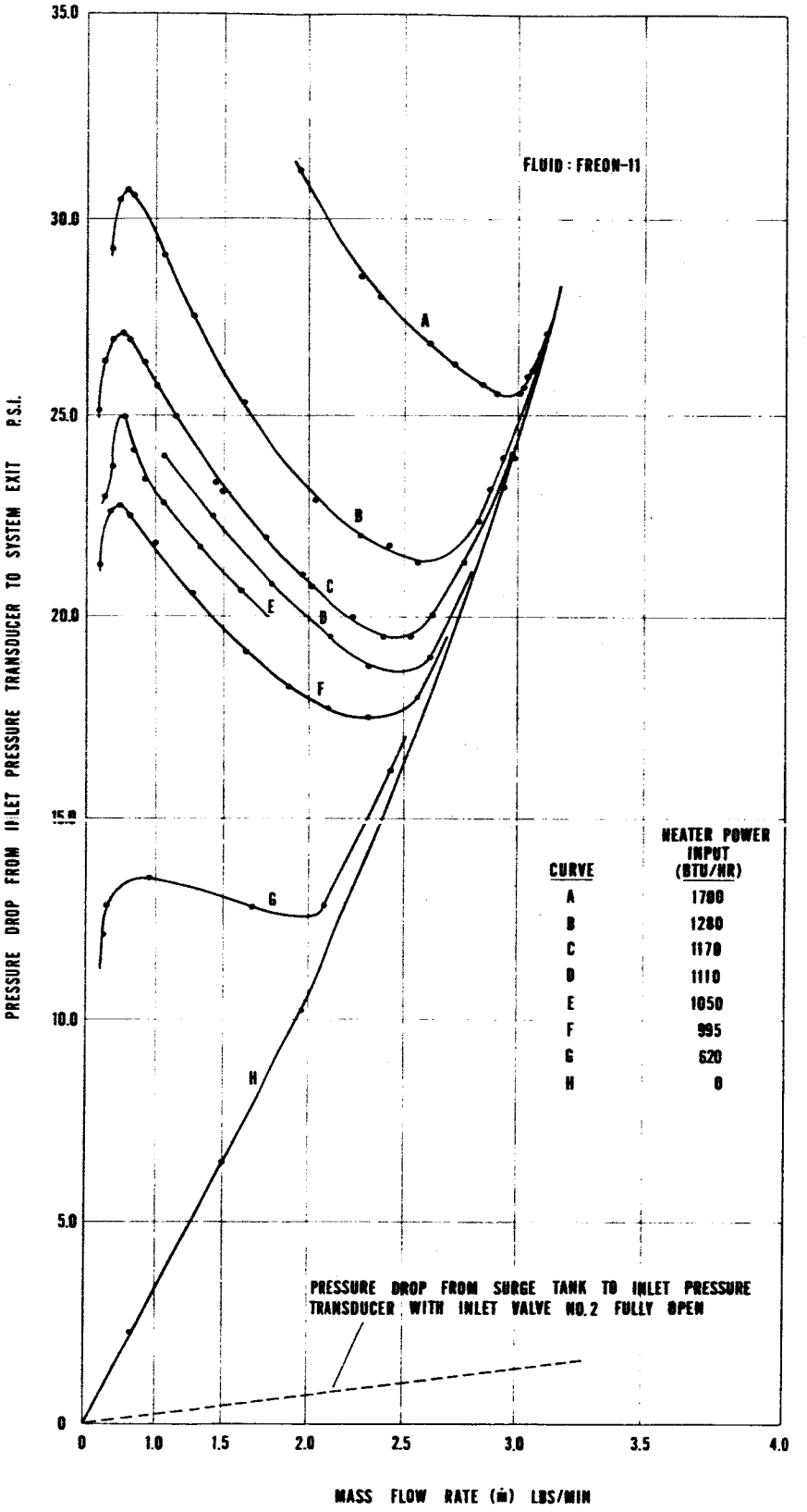

FIG. 5.- PRESSURE DROP VS MASS FLOW RATE STEADY STATE RELATIONSHIP

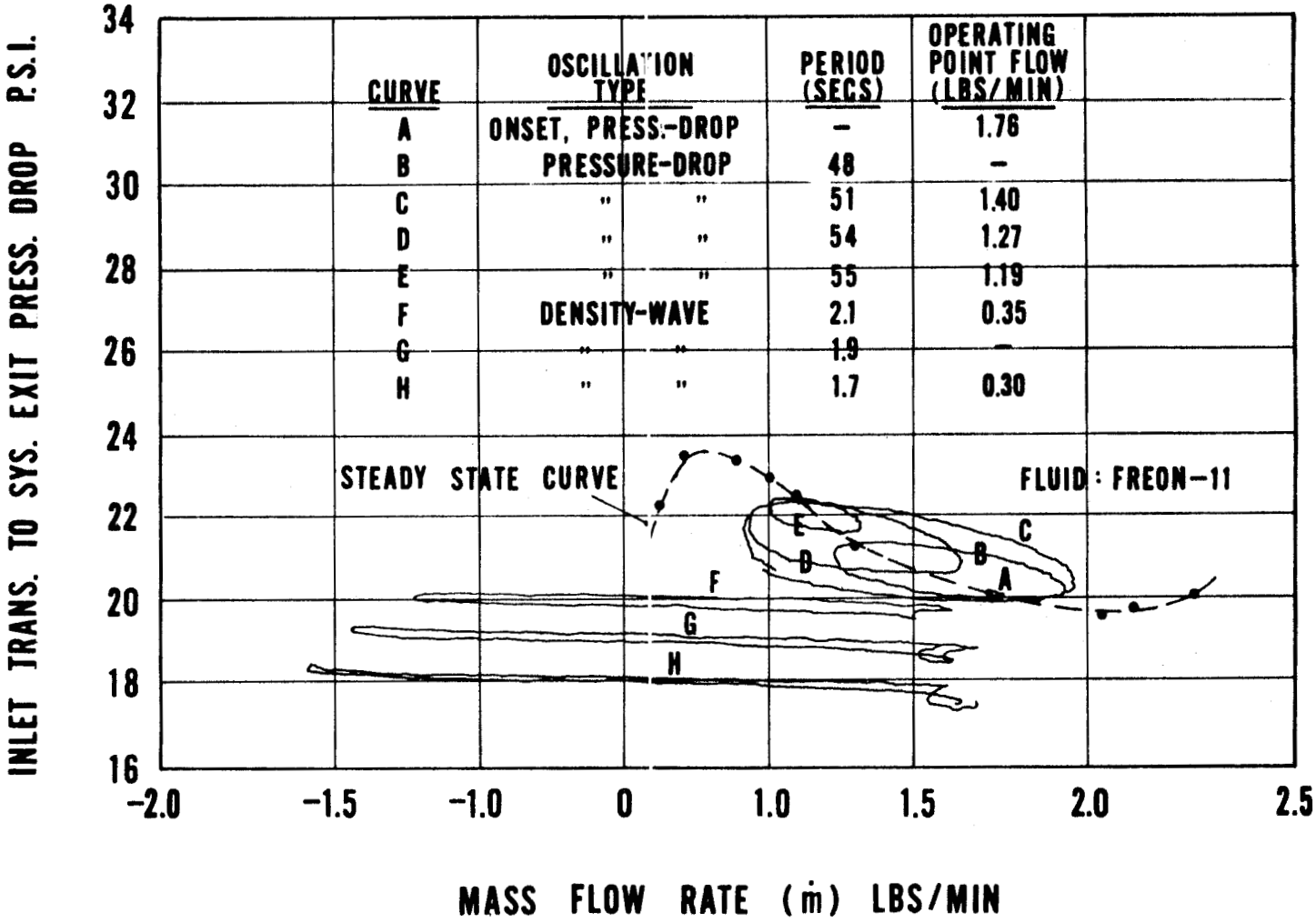

FIG. 6.– PRESSURE DROP VS MASS FLOW RATE LIMIT CYCLES FOR HEAT INPUT OF 1015 BTU/HR

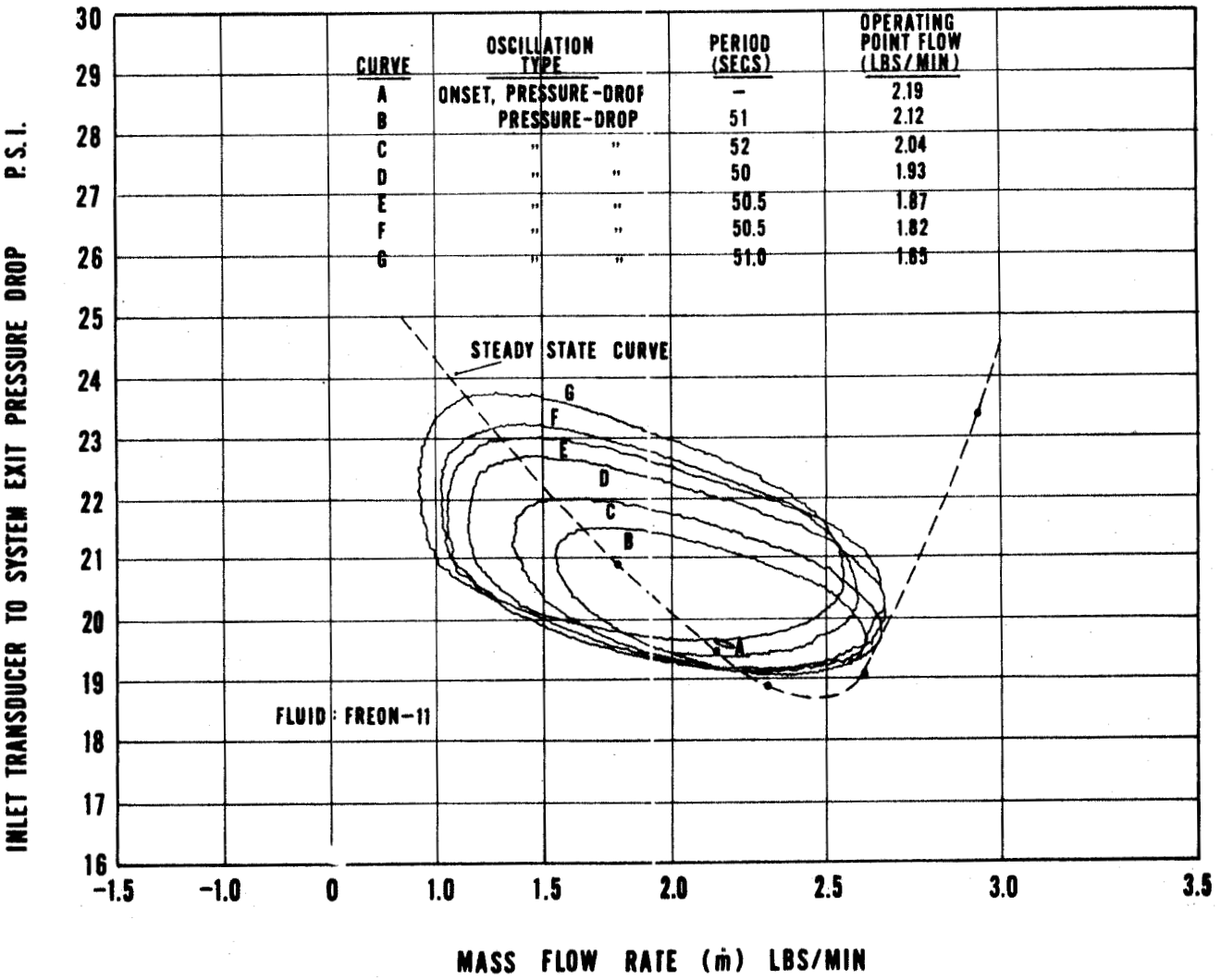

FIG. 7.– PRESSURE DROP VS MASS FLOW RATE LIMIT CYCLES FOR HEAT INPUT OF 1110.0 BTU/HR

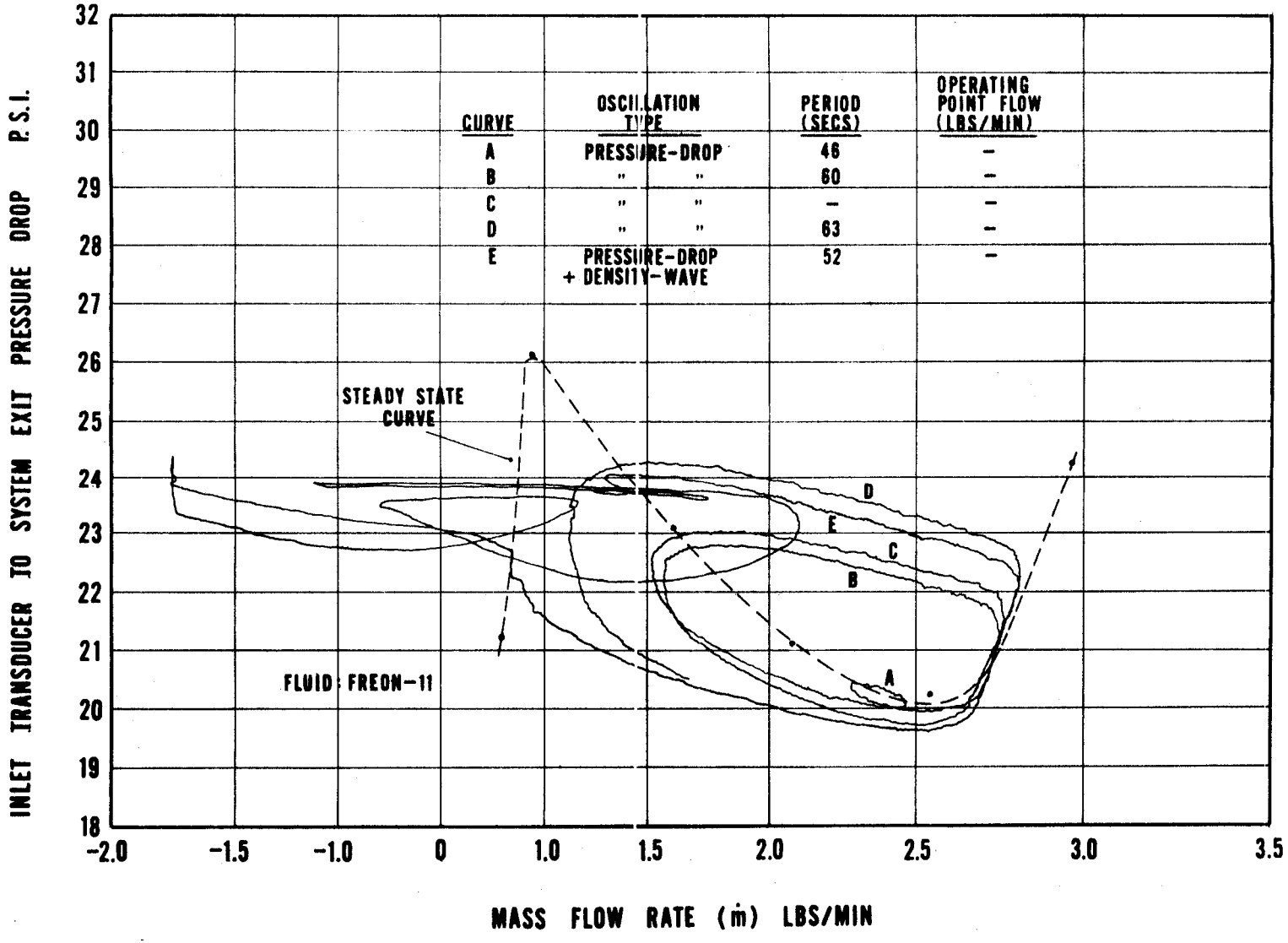

FIG.8.– PRESSURE DROP VS MASS FLOW RATE LIMIT CYCLES FOR HEAT INPUT OF 1170 BTU/HR

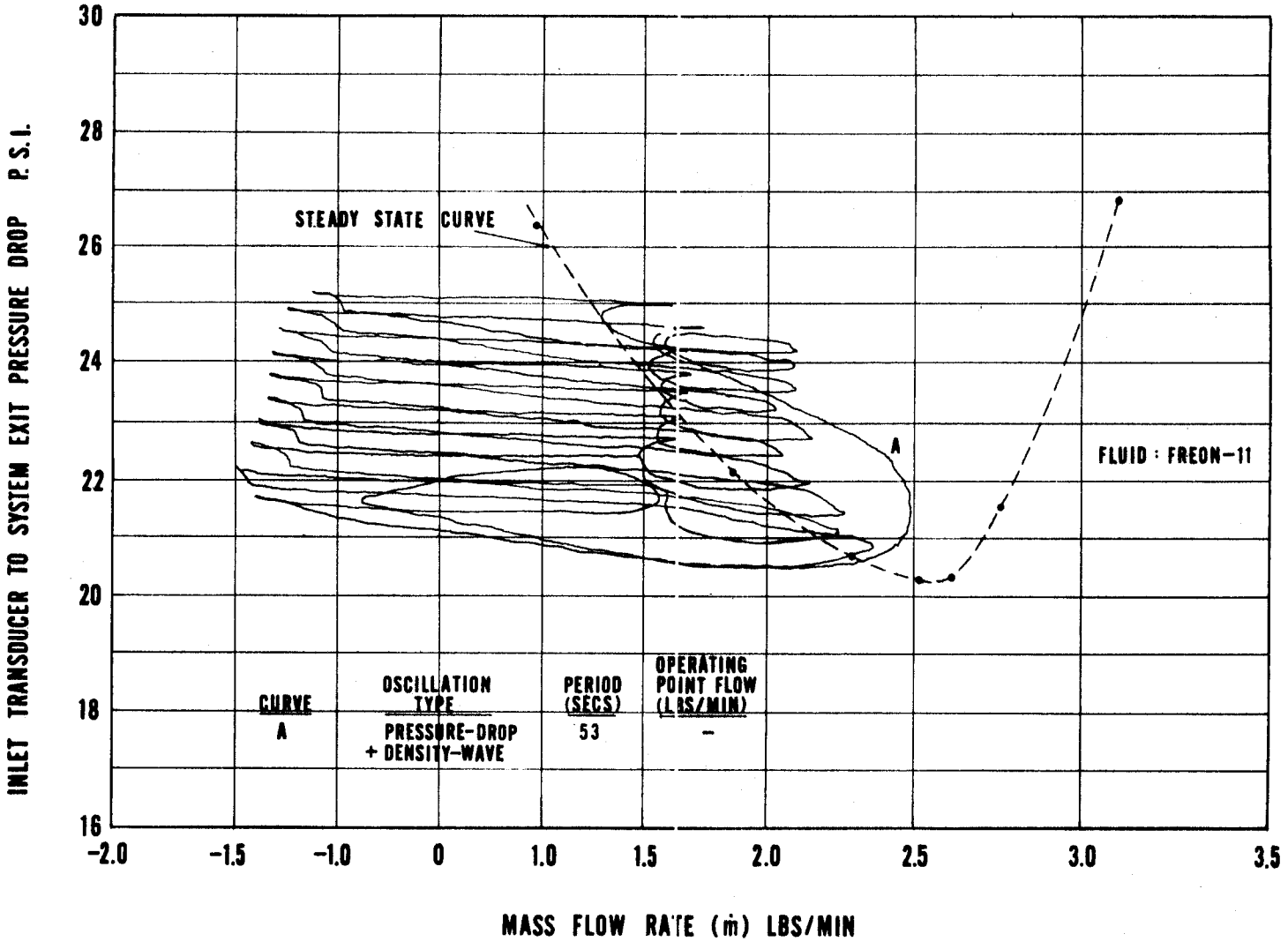

FIG.9.– A COMPOSITE PRESSURE DROP VS MASS FLOW RATE LIMIT CYCLE FOR HEAT INPUT OF 1170 BTU/HR

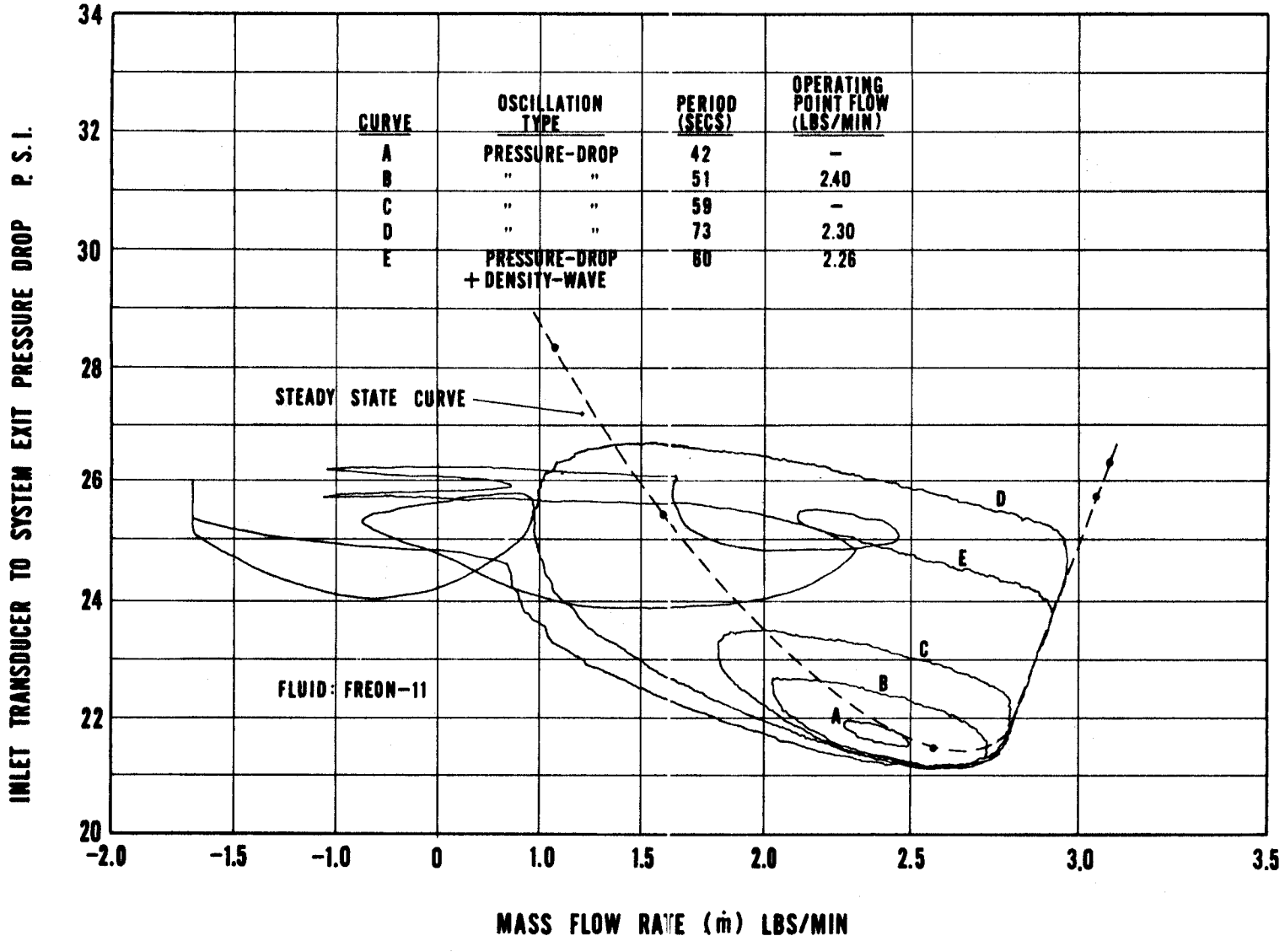

FIG.10.– PRESSURE DROP VS MASS FLOW RATE LIMIT CYCLES FOR HEAT INPUT OF 1280 BTU/HR

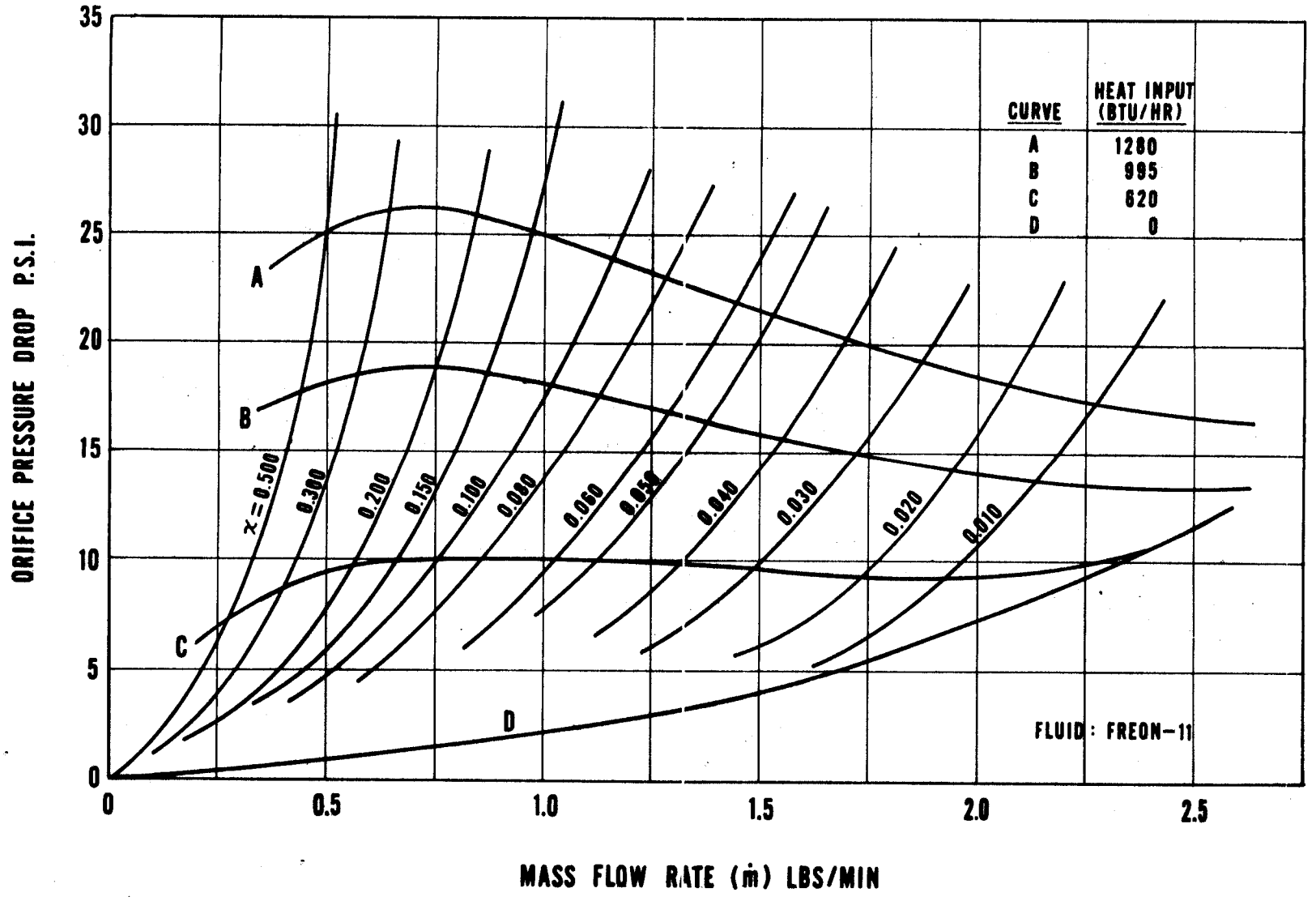

FIG.11.– ORIFICE PRESSURE DROP VS MASS FLOW RATE FOR TWO-PHASE FLOW

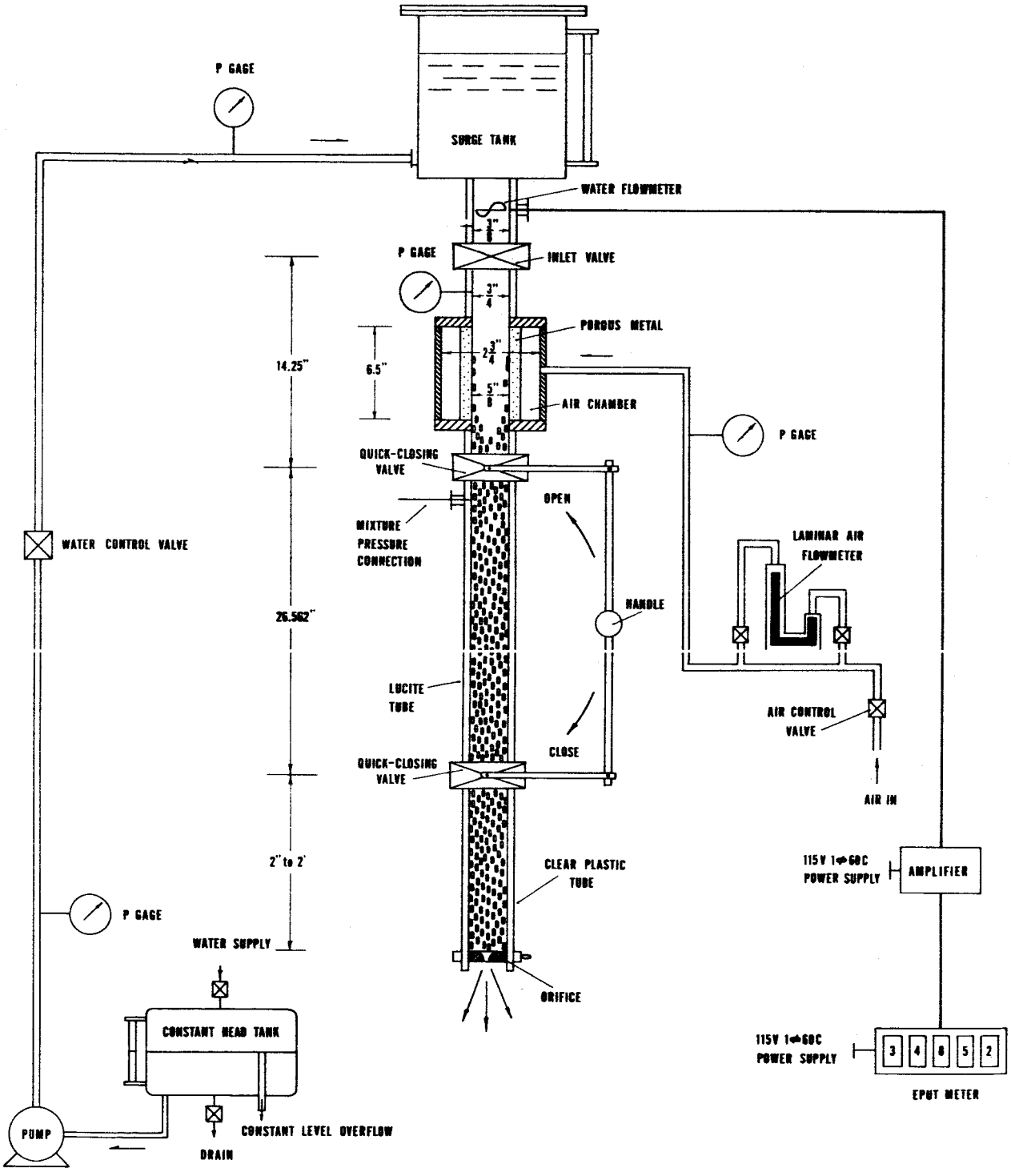

FIG. 12. – SCHEMATIC DIAGRAM OF EXPERIMENTAL SET-UP FOR SLIP INVESTIGATION

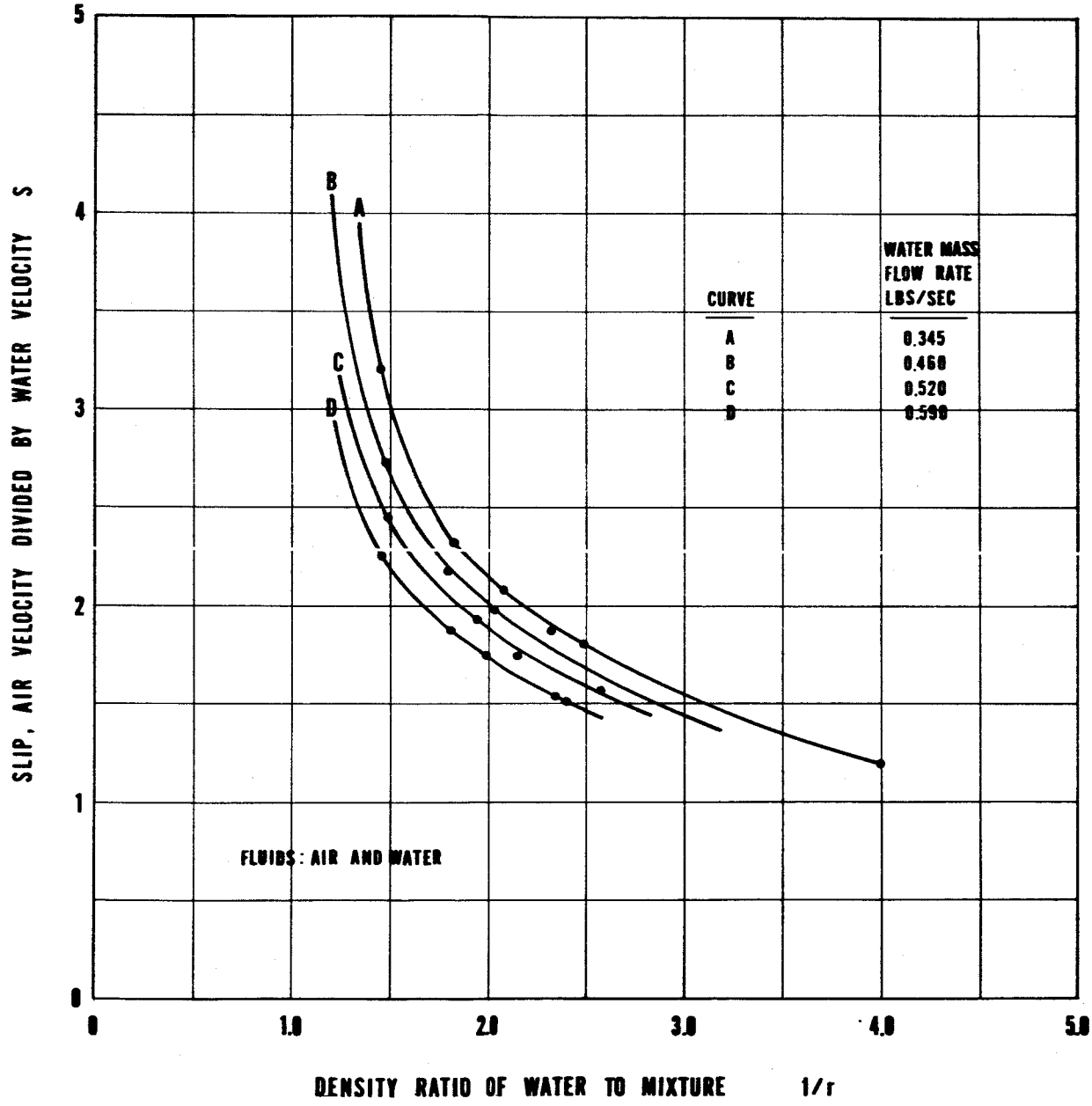

FIG. 13.– SLIP VS DENSITY RATIO

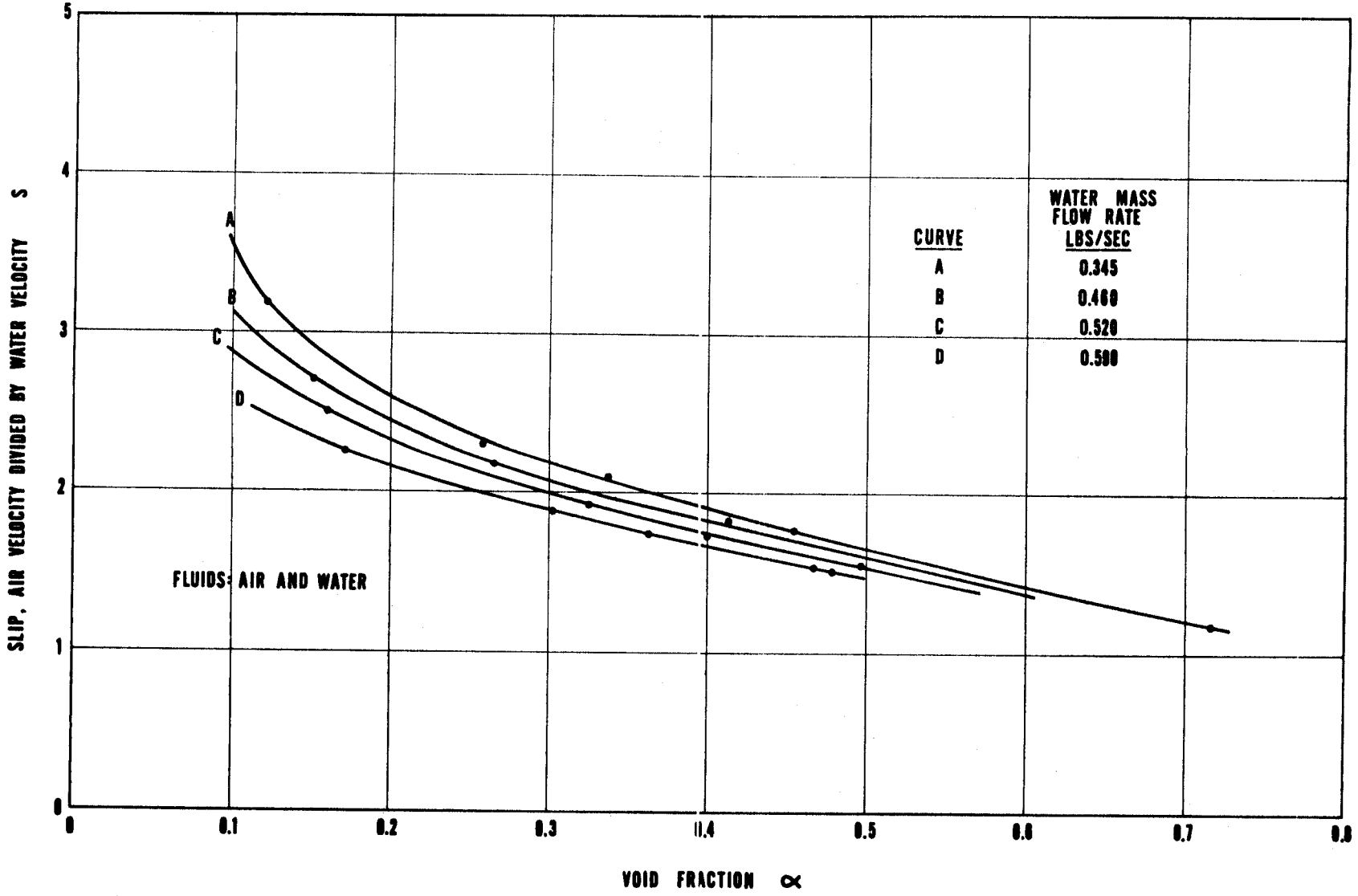

FIG. 14.– SLIP VS VOID FRACTION